ARTICLE

Evaluation of the effects of climate change on forest watershed hydroecology using the RHESSys model: Seolmacheon catchment

Hyungjin Shin[1] · Minji Park[2] · Jiwan Lee[3] · Hyeokjin Lim[4] · Seong Joon Kim[3]

Abstract

This study examines the effects of future climate changes on watershed hydroecology, including runoff, evapotranspiration, soil moisture content, gross primary production (GPP), and photosynthetic productivity (PSNnet), by applying the Regional Hydroecological Simulation System model to the Seolmacheon catchment (8.5 km^2). Based on the daily runoff, evapotranspiration, and soil moisture content in the watershed from 2007 to 2009, calibration (2007–2008) and validation (2009) of the model were conducted. By utilizing PSNnet and GPP data collected with the Moderate Resolution Imaging Spectroradiometer sensor onboard the Terra satellite, model calibration (2007) and validation (2008) were implemented. For future climate change data, the MIROC3.2 (hires) and the HadCM3 climate change scenarios (A1B and B1), which were provided by the IPCC, were used for reference. Compared to the baseline period, the future temperature increased by a maximum of +4.9 °C in the MIROC3.2 A1B scenario, and precipitation increased substantially in spring and winter. In the hydrological evaluation, MIROC3.2 showed annual change rates from −33.9 to 6.0%. Both the A1B and B1 scenarios showed 6.0% and 1.0% increases in the 2020s and −33.9% and −32.8% decreases in the 2080s, respectively. For HadCM3, the A1B (B1) scenario showed rates of −9.9% (1.4%), −48.6% (−19.2%), and −42.4% (−32.1%), in the 2020s, 2050s, and 2080s, respectively. Because climate region movement is relatively slow for temperature ranges when plant movement increases, existing forests might survive in their minimum state or vanish under extreme conditions, such as heat stress, droughts, and fires. In the simulation, the evapotranspiration volume, which was closely related to vegetation, caused the average annual temperature to increase by 2.6–3.6 °C, which caused local vegetation to vanish.

Keywords Climate change · RHESSys · Soil moisture · Evapotranspiration · Streamflow · PSNnet · GPP

Introduction

On February 2, 2007, the United Nations Intergovernmental Panel on Climate Change (UN IPCC) released its comprehensive report on climate change 6 years following the previous meeting, which noted that global warming has resulted from human activity and that the temperature of Earth's surface would increase by as much as 1.8–4.0° within this century. The report also warned that such climate changes would result in more serious heavy rains, ice melting, droughts, scorching summer heats, and sea level increases (IPCC 2007). Temperature increases and changes in precipitation patterns in the future due to global warming will lead to changes in evapotranspiration and soil moisture content and, ultimately, changes in the water cycle and runoff (Minville et al. 2009; Shi et al. 2011; Dan et al. 2012). As a result, a serious will arise regarding water resources, including stream flow rates, the aquatic ecosystem, agriculture, floods, droughts, and water quality. Therefore, it is necessary to predict and evaluate the effects of climate changes on water resources for long-term and national water resource plans (Yang et al. 2009; Joh et al. 2011; Shi et al. 2013; Park et al. 2013; Shin et al. 2014).

✉ Seong Joon Kim
kimsj@konkuk.ac.kr

1. Rural Research Institute, Korea Rural Community Corporation, Ansan-si, South Korea

2. Han River Environment Research Center, Yangpyeong-gun, Gyeonggi-do, South Korea

3. Department of Civil, Environmental and Plant Engineering, Konkuk University, 1 Hwayang dong, Gwangjin-gu, Seoul 143-701, South Korea

4. Korea Institute of Hydrological Survey, Goyang-si, South Korea

When simulating and predicting hydrological changes in watersheds throughout ecosystem water cycles, it is known that evapotranspiration affects runoff and soil moisture content significantly, which are in turn affected by climatic states and surface evaporation characteristics, including net radiation, ground and atmospheric temperatures, soil moisture, wind velocity, and air pressure. Hydrological models used in hydrological evaluation studies hardly consider the effects of changes in leaf area index (LAI), stomatal resistance (related to changes in climate and CO_2 density), soil moisture content, evapotranspiration, and streamflow due to mainly insufficient measured data related to evapotranspiration and soil moisture content. Few simulations have been performed regarding the LAI and stomatal resistance. Due to costs when measuring evapotranspiration and soil moisture content and the limited availability of equipment in Korea, there has been limited data on the actual measurement of runoff and hydrological elements. Thus, actual measurement data of hydrological elements (excluding a except for runoff and so on) have been in a referred to in previous study. As a result, there have been few studies on hydrological calibration. However, since 2007, the Hydrological Survey Center at the Korea Institute of Construction Technology has made it possible to measure evapotranspiration and soil moisture contents in the Seolmacheon catchment, and comparable and quality measurements have accumulated. The utilization of actual measurement data is expected to enhance the reliability of the model simulation results (Joh et al. 2010). Few studies have calculated regional or global net production amounts by means of satellite images. The local observation of net production amounts requires a substantial amount of time and effort due to measurement difficulties. By utilizing the Terra MODIS to obtain satellite images over large areas, it is now possible to monitor certain regions (or even national territories) with insufficient information. Net production information can be utilized to examine various factors, such as the carbon cycle, biosphere characteristics (Nemani et al. 2003), and the expected amount of food and plant production (Running et al. 2004). MODIS net production data are obtained with the BIOME-BGC model, which is an ecological model used in the MODIS NPP algorithm and includes input factors such as climate data, land cover rate, MODIS LAI, and the photosynthesis effective radiation amount (Running et al. 2000).

In most hydrological models, potential evapotranspiration that is estimated with a soil moisture content or vegetation empirical formula is utilized to statistically predict actual evapotranspiration. When modeling vegetation changes in a hydrological model, vegetation information (e.g., LAI and stomatal resistance) used for evapotranspiration estimation is of great importance. Among the ecology and hydrological process studies that have used watershed hydroecology models, the Sim-CYCLE terrestrial ecosystem model (Ito and Oikawa

2000) refers to potential evapotranspiration rates that explain soil moisture content changes related to photosynthesis. The Frankfurt biosphere model (Lüdeke et al. 1994) and CEVSA model (Cao and Woodward 1998), which utilize a similar approach regarding the potential evapotranspiration and soil moisture content empirical formula, calculate streamflow as the remaining quantity when the soil moisture reaches full capacity. In addition to the BIOME-BGC, RHESSys is a more comprehensive ecology model that is capable of comparatively examining crown layer blocking and evapotranspiration in a hydrological cycle. Recently, Topog (Vertessy et al. 1996) and Macaque (Watson et al. 1999) hydrological models have made it possible to simulate detailed carbon changes and hydrological elements related to vegetation growth. For both vegetation and hydrology, most hydrological models (except the few models listed above) can represent neither changing elements nor vegetation parameters.

RHESSys is a type of biogeochemical model used in ecology, but it is different from other models in that it comprehensively simulates the hydrological and biogeochemical cycles. RHESSys simulates the flows of carbon, water, and nutrient salt in three-dimensional space by utilizing a geographic information system (Tague and Band 2004). The distribution of soil moisture contents in a watershed affects the variety of vegetation, primary productivity, and spatial heterogeneity of the soil biogeochemical process, especially for runoff in a forest watershed. For research on the adjusted spatial distributions of various soil moisture conditions for grassland productivity, RHESSys has been applied to forest watersheds in the northwest region of the Pacific (Tague and Band 2001) and the northern plains of Canada (Creed et al. 2000). Zierl et al. (2006) applied RHESSys to various small watersheds over the Alps in Europe and, as a result, was able to predict evapotranspiration, runoff, and snowfall amounts that were significantly similar to the actual measurements. Hwang et al. (2008) applied RHESSys to the Gwangneung research watershed and comparatively analyzed runoff, soil moisture content, evapotranspiration, and net ecosystem exchange data. López-Moreno et al. (2014) predicted the future increase in water storage with RHESSys to manage the water volume in reservoirs across Spain to reflect climate changes.

The purpose of this study is to analyze the effects of future climate changes on hydrological patterns (runoff, evapotranspiration, soil moisture content) and ecological circulations over forest watersheds.

Materials and methods

Study area and watershed

To apply a hydroecology model in this study, the Seolmacheon catchment upstream of the Imjin River was chosen

of which hydrological elements have been observed and available for a prolonged period since 2007 by the Korea Institute of Construction Technology for the observation of hydrological elements (Korea Institute of Construction Technology 2008). For hydrological observations of the watershed, six precipitation stations (Jeonjeokbigyo, Biryongpodae, Beomryunsa, Beanbay, Seolmari, and Gammasan), one water level station (Jeonjeokbigyo), and one weather observation station (Biryongpodae) were established for observations at 10-min intervals. The flux tower and the soil moisture contents were regularly observed over the deciduous forest region, which is located between 126° 52′–126° 58′ E and 37° 55′–37° 58′ N (Fig. 1). The watershed area is 8.5 km^2, its basin length is 5.8 km, its channel slope is 2%, and its average annual precipitation is 1210 mm. This catchment is a typical steep-slope, mountainous meandering stream, where 90% of the watershed consists of coniferous trees and broadleaf trees that are 20–30 years of age. The topsoil is thin, and the recharge capacity is very low. A large quantity of rocks and gravel on the slope can cause debris flow due to torrential downpours.

RHESSys model description

RHESSys was designed to comprehensively predict the cycles and movements of water, carbon, and substances within a watershed related to plants, air, and soil. As driving factors, changes in the hydrologic process, including runoff, soil moisture content, and evapotranspiration, along with biogeochemical processes, including tree increments, net primary productivity, soil aspiration, and the LAI, can be predicted on a daily basis (Tague and Band 2004). Earlier versions of RHESSys were designed to combine the forest biogeochemical cycle (FOREST-BGC) canopy model (Running and Coughlan 1988) with topographical patterns due to critical meteorological forcing (Running et al. 1987); the model (Fig. 2), which was developed by Band et al. (1993) (Baron et al. 1998; Tague and Band 2004), then integrated the hydrological process by adopting the TOPMODEL hydrological model (Beven and Kirkby 1979) and the mountainous micrometeorology model MTCLIM (Running et al. 1987).

Unlike coupled models, RHESSys describes the water connectivity between landscapes and vertical water flows directly. The model also describes the interactions among the carbon and substance cycles in an ecosystem, including the hydrological process and plant growth. Hence, this method is advantageous as it can classify and specifically evaluate processes such as photosynthesis and evapotranspiration, as well as the physical characteristics of detail procedures. The Farquhar model (Farquhar and von Caemmerer 1982) calculates photosynthesis based on the limitations of three elements, which are used to calculated photosynthesis: enzyme (nitrogen), electronic transmission (light), and pore conductivity (light and water). For the calculation of potential evaporation, the Penman–Monteith expression (Monteith 1965) is applied. Stomatal conductance utilizes the Jarvis multiplicative model (Jarvis 1976) assuming that various environmental limitations (e.g., radiation, CO_2, leaf water potential, and vapor pressure
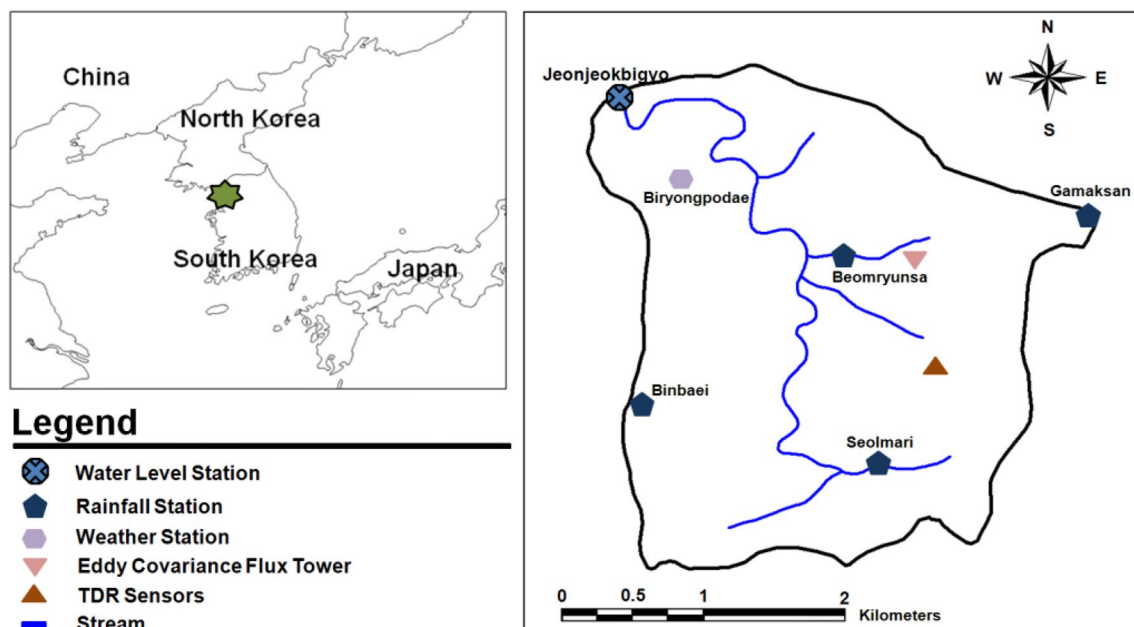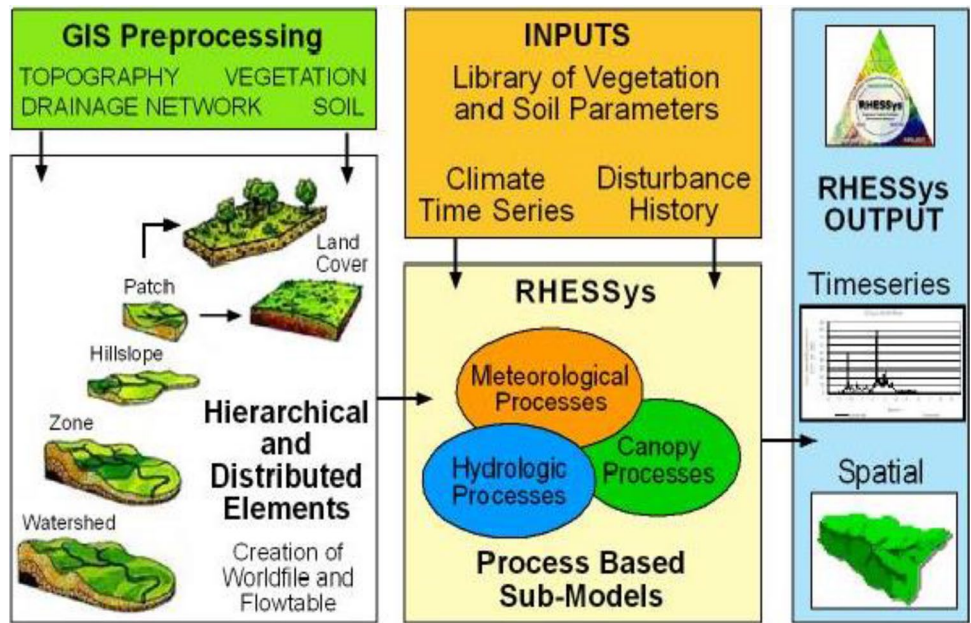

Fig. 1 Map of the Seolmacheon watershed and locations of the hydrological observation sites

Fig. 2 The structure of the RHESSys model. (Tague and Band 2004)

deficit) are determined with the maximum stomatal conductance (Jarvis 1976), which expands the range of hydraulic conductivity by using LAI information. Photosynthesis and evapotranspiration share values of hydraulic conductivity. Both RHESSys and BIOME-BGC utilize the CENTURY model to express soil organic matter decomposition, and RHESSys uses CENTURYNGAS (Parton et al. 1996) to simulate *N*-cycling processes, such as nitrification and denitritation. The RHESSys model, which is a watershed hydroecology model that considers hydrologic

and ecological processes, was applied to the Seolmacheon catchment (Fig. 3).

Future climate change scenarios

This study uses the MIROC3.2 (hires) and the UKMO HadCM3 A1B and B1 scenarios to extract monthly average temperature (°C) and precipitation deviations (%) in the future (2009–2100) using a baseline of 1977–2006, where the 100 future years are divided into three analysis periods
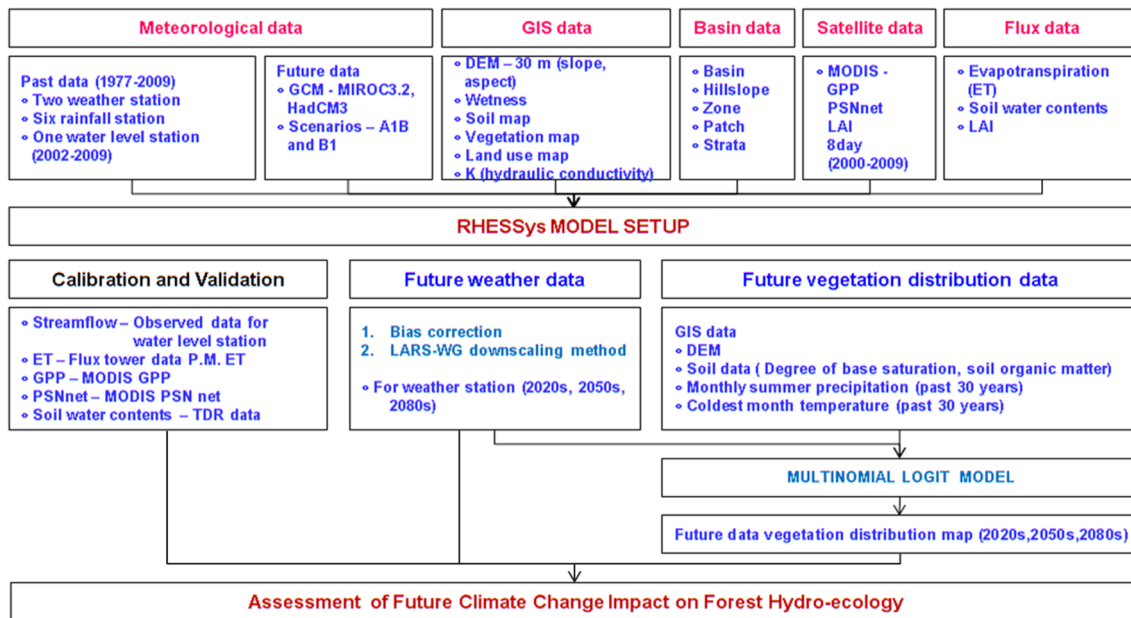

Fig. 3 Flowchart of this study

in increments of 30 years (i.e., 2020s: 2010–2039; 2050s: 2040–2069; and 2080s: 2070–2099), to produce climate change scenarios for each observation center based on 100-year daily data developed by the LARS-WG. Shin et al. (2014) presents a detailed description of this process.

After the period is divided into 30-year units, MIROC3.2 A1B temperature increases for spring, summer, fall, and winter from $+3.6\%$ (0.4 °C) to $+28.8\%$ (3.2 °C), $+4.6\%$ (1.0 °C) to $+17.7\%$ (4.2 °C), $+18.0\%$ (2.3 °C) to $+47.8\%$ (6.1 °C), and $+130.4\%$ (3.1 °C) to $+256.9\%$ (6.0 °C), respectively. MIROC3.2 A1B precipitation increases for precipitation 2020s, and 2080s from 10.2% (129.7 mm) to 23.1% (292.3 mm) (Table 1, Fig. 4).

Input and measured data for the RHESSys model simulation

To evaluate the applicability of the RHESSys model, a distribution model in this study based on hydrological climate data has been determined using a validated/calibrated database from 2007 to 2009, which includes a digital elevation model (DEM), a soil map and land use, vegetation, satellite, daily precipitation (mm), solar radiation (MJ/m^2), average wind velocity (m/s), and average relative humidity (%) data (Table 2). Because it is currently operated as a model watershed by the Korea Institute of Construction Technology (1995-present), the Seolmacheon catchment has a precipitation station, gauging station, flux tower, soil moisture content measurement system, and weather observation station to collect hydrological data. For this study, data from the Seolmacheon

catchment, including hydrological data, evapotranspiration data, and soil moisture content, were provided from the hydrological survey center at the Korea Institute of Construction Technology and used for model validation/calibration. The evapotranspiration validation and calibration were based on the measurements by using the flux tower eddy covariance system for mixed forests. For the soil moisture content calibration and validation, measurements were utilized by using time domain reflectometry (TDR) sensors in the Seolmacheon catchment sandy loam soil (Deoksan Toyangtong) and runoff data collected at the watershed entrance. These hydrological elements were all actual measurements collected by the Hydrological Survey Center at the Korea Institute of Construction Technology. Regarding evapotranspiration, the post-treated and calibrated data (Kwon et al. 2009) were presented by the Yonsei University Department of Atmospheric Sciences. The climate condition input data were accumulated from 2002 to 2008.

For vegetation distributions, a forest type map produced by the fourth national forest resources inventory survey (conducted by the Korea Forest Service) was used and reclassified for three forest types—coniferous forests (with a crown occupied area and a vegetation stock ratio of 75% or greater), deciduous forests, and rocky areas—that are used in the hydrological and environmental management area. The flow rates were defined using hydraulic conductivity. Hence, the water flow characteristics in the soil can be interpreted regarding the hydraulic conductivity. In this study, the saturated hydraulic conductivity from Clapp and Hornberger (1978) was utilized as the model input data.

Table 1 Annual and seasonal precipitation and temperature change rates (%)

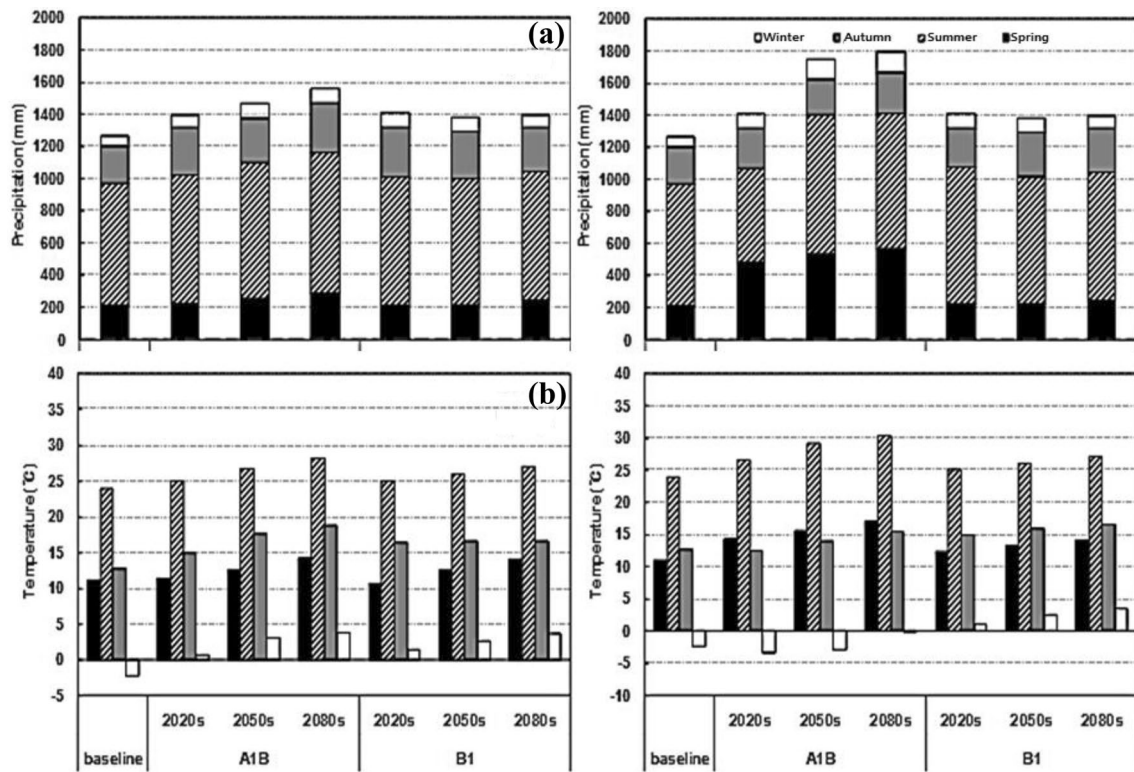| Period	2020s				2050s				2080s			
GCM	MIROC3.2		HadCM3		MIROC3.2		HadCM3		MIROC3.2		HadCM3	
Scenario	A1B	B1	A1B	B1	A1B	B1	A1B	B1	A1B	B1	A1B	B1
Spring (March–May)												
Prec.	8.1	2.5	133.9	8.9	21.1	3.6	154.4	7.9	37.8	16.0	170.6	16.0
Temp.	3.6	−3.5	29.0	11.7	13.8	13.8	41.7	20.2	28.8	27.9	54.0	27.9
Summer (June–August)												
Prec.	4.5	4.7	−23.8	11.0	11.4	2.9	14.0	4.1	14.7	5.3	10.7	5.3
Temp.	4.3	3.9	10.9	5.0	11.6	8.3	21.5	8.6	17.7	12.9	26.7	12.9
Autumn (September–November)												
Prec.	27.8	32.3	6.7	7.2	20.5	26.3	−2.9	18.6	33.7	18.8	9.5	18.8
Temp.	18.0	29.7	−2.0	17.1	37.9	30.8	10.1	25.0	47.8	30.3	21.9	30.3
Winter (December–February)												
Prec.	21.4	38.6	36.0	32.7	38.4	35.8	84.1	36.2	35.9	18.0	100.5	18.0
Temp.	130.4	157.0	−41.0	143.6	225.9	208.7	−25.1	207.0	256.9	250.9	92.9	250.9
Annual												
Prec.	10.2	11.1	11.0	11.1	16.1	9.0	37.8	9.0	23.1	10.2	41.6	10.2
Temp.	15.0	17.7	10.1	17.7	31.8	27.2	23.0	27.2	43.1	35.1	38.2	35.1

Fig. 4 Future downscaled yearly precipitation (**a**) and temperature (**b**) in the 2020s, 2050s and 2080s for the A1B and B1 scenarios (left: MIROC3.2; right: HadCM3)

Table 2 Data sets for RHESSys model parameterization

Data type	Source	Scale/period	Data description/properties
Topography	Korea National Geography Institute	1/5000	Elevation
Soil	Korea Rural Development Administration	1/25,000	Soil classifications and physical properties such as bulk density, texture, porosity, wilting point, field capacity and saturated hydraulic conductivity
Land cover	Landsat TM satellite image	30 m	Land cover classifications such as water, forest, urban, grassland, bare ground, paddy and upland crop
Vegetation information	Ministry of Environment	30 m	Forest classification (3 classes)
Weather	Korea Meteorological Administration	1977–2009	Daily precipitation, mean, max., min., temperature, wind speed, relative humidity and sunshine hour
Streamflow	Korea Institute of Construction Technology	2007–2009	Daily observed streamflow
Evapotranspiration	Korea Institute of Construction Technology/ Yonsei Univ.	2007–2009	Daily evapotranspiration data at mixed forest area
Soil water content	Korea Institute of Construction Technology	2007–2009	Daily soil water content
Photosynthesis	Terra MODIS satellite image	2000–2008	Photosynthetic Productivity (8 days) Gross Primary Production (8 days)

Future forest vegetation changes

To predict changes in future vegetation distributions in forests, a database was established for this study, where current and future climate, altitude, and soil map data over South Korea were collected. An analysis on the correlation between the collected data and the current vegetation distribution was conducted, and variables with the highest correlations were selected. Regarding the distribution of selected variables and the current vegetation distribution, a multinomial logistic regression was implemented to generate a corresponding expression for each forest vegetation category. Based on the

type and source of the future climate data, future changes in forest vegetation distributions were predicted.

As a result of analyzing the correlations among the 14 environment variables as well as forest vegetation (altitude, temperature, precipitation, soil organic matter, and degree of base saturation). Regarding these six variables—forest vegetation distribution, altitude, temperature in cold months, summer precipitation, degree of base saturation, and soil organic matter—a multinomial logistic regression with a 4 km resolution was implemented. As a result, a correlation regression equation was developed for each forest vegetation type (i.e., coniferous tree, broadleaf tree, broadleaf tree mixed forest, mixed forest; Table 3). Regarding cold month temperatures and summer precipitation in the 2020s (2010–2039), 2050s (2040–2069), and 2080s (2070–2099), the multinomial logit regression expressions for each forest vegetation type were applied, and future vegetation distributions in forests were predicted. In comparison with the current states, the broadleaf trees and mixed forests in the 2080s were predicted to increase by as much as 15.4% and 26.7%, respectively, while coniferous trees would decrease by as much as 62.5%. Because the Seolmacheon catchment has a wealth of broadleaf trees, it is predicted that more broadleaf trees will be distributed in the future. Details of the forest vegetation change results of model have been published (Shin et al. 2012a; in Korean with English abstract).

MODIS data

MODIS is a multipurpose sensor that is applicable over marine, ground, and atmospheric areas. It is a major sensor on the NASA Terra Earth Observation System (EOS) satellite, which provides various types of data about the terrestrial biosphere (i.e., atmospheric, ground, and marine areas) using 36 bands (Shin et al. 2010). The NASA EOS Data Gateway provides various satellite images that are produced through the EOS, including MODIS images, which can be divided into subcategories (i.e., the atmosphere, glacier, land, and ocean) for data calibration (Park et al. 2006). It also has spatial and temporal resolutions that are effective for the observation of time/space characteristics over a certain region. MOD17 combines the initial productivity model and remote sensing methods to understand the global carbon cycle by utilizing a 1 km spatial resolution for vegetation and average GPP and PSNnet products (for 8 consecutive days; gC/m^2), which derive from the Terra satellite MODIS sensor (Running et al. 2000; Heinsch et al. 2003).

Model parameters for calibration and validation

For model calibration, daily runoff data from 2007 to 2008 are used in this study. RHESSys performs the calibration using "m," which is the damping ratio for hydraulic conductivity (dependent on depth), and "K," which is the hydraulic conductivity of each soil type depending on the vegetation distribution (Table 4). Regarding changes in streamflow as a function of parameter changes, as the hydraulic conductivity value (i.e., a streamflow-related parameter) increases, the total runoff increases accordingly. For the operation of RHESSys, the initial values of carbon, nitrogen, and humidity content over the vegetation and soil are required. However, because it is difficult to determine all initial values based only on the actual measurements, RHESSys initializes the model by using the spin-up method, where the initial values of a model are determined until the carbon gain is stabilized in the ecosystem. The period for stabilization is 450 years. After the initialized RHESSys was operated from 2002 to 2009, the results were compared with the actual measurements. Details of the calibrated parameters and streamflow results of model calibration and validation have been published (Shin et al. 2012b; in Korean with English abstract).

Parameters that would affect vegetation growth include whole plant mortality (WPM), dry weight LAI (specific leaf area (SLA), m^2/kgC), the leaf C:N ratio, the nitrogen rubisco content in the leaf, and the coefficient distribution of photosynthesis products. Turnover and mortality parameters are used to describe the portion of the plant pools that are either replaced each year or removed through fire or plant death (White et al. 2000). For all deciduous biomes, Leaf and root turnover (1 year) is set to 1.0, indicating that the entire leaf and fine root carbon pools are turned over every year (White et al. 2000). White et al. (2000) set LWT to 0.7 for all woody biomes. WPM (unit: 1 $year^{-1}$; e.g., total tree death rates and pruning) is applied to the upper and lower parts of the ecological carbon repository system that dies and regenerates

Table 3 Relational functions between forest vegetation types and environmental variables

Forest vegetation	Multinomial logistic regression equation					
Coniferous	− 5.8543	− 0.0032 A	− 0.0088 B	+ 0.0066 C	+ 0.0183 D	− 0.1158 E
Deciduous	− 7.6284	− 0.0069 A	+ 0.0728 B	+ 0.0077 C	+ 0.0181 D	+ 0.5555 E
Deciduous mixed	− 6.7188	− 0.0076 A	+ 0.2214 B	+ 0.0090 C	+ 0.0096 D	− 0.3283 E
Mixed	− 7.0664	− 0.0106 A	+ 0.1545 B	+ 0.0073 C	+ 0.0194 D	− 0.1894 E

A Degree of base saturation, *B* Soil organic matter, *C* DEM, *D* Average summer precipitation over 30 years (i.e., the rainfall variable), *E* Average temperature in cold months over 30 years

Table 4 The streamflow parameters of the calibrated RHESSys model

Parameter	Description	Units	Default	Min. value	Max. value
K Rawls et al. (1982)	Saturated hydraulic conductivity at surface	m/day	1	0.02	5
m	Decay of saturated hydraulic conductivity with saturation deficit	1/(meter of water)	1	0.01	10
porosity_0	Porosity at soil surface	Range (0–1)	0.435	0.395	0.500
porosity_decay	Porosity scaling parameter with depth—porosity decays as	1/m	4000	1	1000
m_z	Decay of saturated conductivity with actual soil depth. If porosity does not scale with depth then m_z should be m/porosity_0	1/m	1	0.5	2

every year (Table 5). The forest values applied to the model (0.005), which are considered to indicate the branch and tree death rates, are based on a large-scale field experiment conducted by forestry researchers. The decrease in transpiration and the increase in carbon absorption (when there is an increase in CO_2) increase both the humidity and soil moisture content. Many researchers state that the increase in CO_2 results in high soil moisture content levels (Knapp et al. 1996; Fredeen et al. 1997; Lutze and Gifford 1998; Morgan et al. 1998; Volk et al. 2000). Maximum stomatal conductance (gsmax; m/s) determines conductivity rates when there are no environmental condition limitations. Three reports have presented the same value of gsmax, which indicates a minimal difference among natural vegetation from that perspective (Kelliher et al. 1995; Körner 1995; Schulze et al. 1994). Kelliher et al. (1995) performed a more recent evaluation on all types of biomasses, where a gsmax of 0.006 m/s was applied. The LAI significantly affects all aspects of canopy physiology and is considered when calculating SLA and leaf carbon (kgC/m^2) production.

Results and discussions

Results of the hydrological calibration and validation

As objective functions of the model, the Nash–Sutcliffe (Nash and Sutcliffe 1970) model efficiency and coefficients of determination were used. Based on the average parameter values and daily runoff data from 2007 to 2008, the model validation was conducted. After analyzing the correlations among the actual measurements and the simulated measurements for daily runoff during the calibration period at the watershed entrance, the Nash–Sutcliffe model efficiencies were 0.63 and 0.84, and the coefficients of determination were 0.74 and 0.92, respectively, indicating high correlations (Table 6).

For the simulated results for runoff, evapotranspiration, and soil moisture content, daily soil moisture contents recognized by the TDR sensor were compared with those that were predicted with the RHESSys model, and the results are shown in Table 5 and Fig. 5. The predicted soil moisture contents in summer, which is a season of growth, were quite similar to those from the actual measurements. However, the predicted values using the RHESSys model simplified and overestimated the daily changes in comparison with the actual measurements.

Table 5 The ecophysiological parameters of the calibrated RHESSys model (White et al. 2000)

Parameters	Description	Units	DBF	ENF
epc.gl_smax	Maximum stomatal conductance	m/s	0.006	0.006
epc.proj_epc.proj_sla	Specific leaf area	m^2/kgC	32.0	8.2
epc.leaf_cn	Carbon:nitrogen ratio of leaves	kgC/kgN	25.0	42.0
epc.froot_turnover	Annual fine root turnover fraction (percent carbon per year)	Range (0–1)	1.00	0.26
epc.livewood_turnover	Annual live wood turnover fraction (percent carbon per year)	Range (0–1)	0.70	0.70
epc.mortality	Vegetation loss through mortality	Range (0–1)	0.01	0.005
epc.froot_cn	Carbon:nitrogen ratio for fine roots	kgC/kgN	48.0	58.0
epc.alloc_frootc_leafc	Ratio of new fine root carbon to new leaf carbon allocation	Dimensionless	1.2	1.4

DBF deciduous broadleaf forest, *ENF* evergreen needle leaf forest

Table 6 Hydrological calibration and validation results (Shin et al. 2012b)

Period	Observation			Simulation		Statistical summary		Note
	P (mm/y)	Q (mm/y)	QR (%)	Q (mm/y)	QR (%)	E	R^2	
2007	1262.2	761.0	0.60	736.4	0.58	0.59	0.59	C
2008	1498.3	941.6	0.63	1103.2	0.74	0.67	0.89	C
2009	1351.7	1001.4	0.74	831.8	0.62	0.84	0.92	V
Period	P	SM (%)				ET (mm)			Note
		Period	Obs.	Sim.	R^2	Period	Obs.	Sim.	R^2	
2007	1262.2	Jun.–Dec.	26.0	25.6	0.37	Sep.–Dec.	109.0	113.5	0.53	C
2008	1498.3	Jun.–Dec.	22.9	25.0	0.52	Jan.–Dec.	471.7	473.8	0.54	C
2009	1351.7	Jun.–Dec.	23.6	21.5	0.18	Jan.–Dec.	408.6	471.0	0.49	V

P precipitation, Q streamflow, QR runoff ratio, SM soil moisture, ET evapotranspiration, E Nash–Sutcliffe model efficiency, R^2 coefficient of determination, C calibration, and V verification

In general, hydrological models require validation and calibration regarding simulated and actual measurements of daily runoff due to observation data limitations. In contrast, this study utilizes hydrological data, PSNnet, GPP ecological data for runoff, evapotranspiration, and soil moisture content for model validation and calibration in comparison with the observation and remote sensing data. Hydrological and ecological parameters organically affect each other. Specifically, transpiration in plants is a process where soil moisture circulates in woody tissues and leaves through the roots, which affects soil moisture content loss and is a deciding factor for runoff in watersheds. This observation and other major parameters that affect ecology are presented in Table 5. For evapotranspiration, the daily evapotranspiration measured at the flux tower was compared with that of the RHESSys model.

Modeled evapotranspiration contains an interception measurement related to evaporation, as well as the vegetation crown canopy, snow sublimation, and vegetation transpiration volume, which are calculated based on the daily precipitation occurrence time and the vapor pressure deficit (VPD). Therefore, evapotranspiration is affected significantly by soil moisture and transpiration volume, which are closely related to ground and vegetation water flow.

Results of the ecological parameter calibration and validation

When using the Terra satellite MODIS sensor with a 1 km resolution for vegetation, the average daily production results for the 8-day GPP (gC/m^2) and PSNnet (gC/m^2) were compared with those simulated by the model. For PSNnet, the coefficients of determination after calibration (2007) and validation (2008) were 0.55 and 0.38, respectively. MODIS PSNnet showed overestimated values compared to the expected values from the RHESSys model. For GPP,

the RHESSys model expected value was overestimated, and the simulated monthly pattern showed a similar tendency. The coefficients of determination after calibration (2007) and validation (2008) were 0.93 and 0.93, respectively. The simulated results from the watershed model are presented in Table 7. PSNnet and GPP excluded transpiration activities during precipitation in the model, as was the case for evapotranspiration as well. Hence, the PSNnet values in July and August, which comprise the summer season with a substantial amount of precipitation, were lower than those in May. The simulated values were lower than the MODIS values measured with remote sensing.

The effects of future climate and forest vegetation changes on forest hydrological conditions

First, annual and seasonal changes in evapotranspiration (Fig. 6a) show a decrease in annual evapotranspiration and a general decrease over all seasons. MIROC3.2 changed throughout the year from −33.9 to 6.0%. Both the A1B and B1 scenarios showed an increase from 1.0 to 6.0% in the 2020s but a decrease from −32.8 to −33.9% in the 2080s. For seasonal evapotranspiration values in every scenario, winter evapotranspiration increased by 99.4%, while that in spring and summer decreased by −39.7% and 40.7%, respectively. Evapotranspiration in fall increased only in the 2020s, based on the annual comparison, and decreased to −26.8% throughout the rest of the period. For HadCM3, the change rates in the A1B scenario were −9.9%, −48.6%, and −42.4% in the 2020s, 2050s, and 2080s, while those in the B1 scenario were 1.4%, −19.2%, and −32.1%, respectively. For seasonal evapotranspiration values, the B1 scenario in spring was −38.8% in the 2080s, which was the largest negative rate, and that in the B1 scenario was −3.4% in the 2020s, which was the smallest negative rate. In summer, the rate decrease was consistent in the MIROC3.2 data, and

Fig. 5 Simulated and observed daily streamflow (**a**), evapotranspiration (**b**), soil water content (**c**), PSNet (**d**) and GPP (**e**) from 2007 to 2009 (Shin et al. [2012b](#))
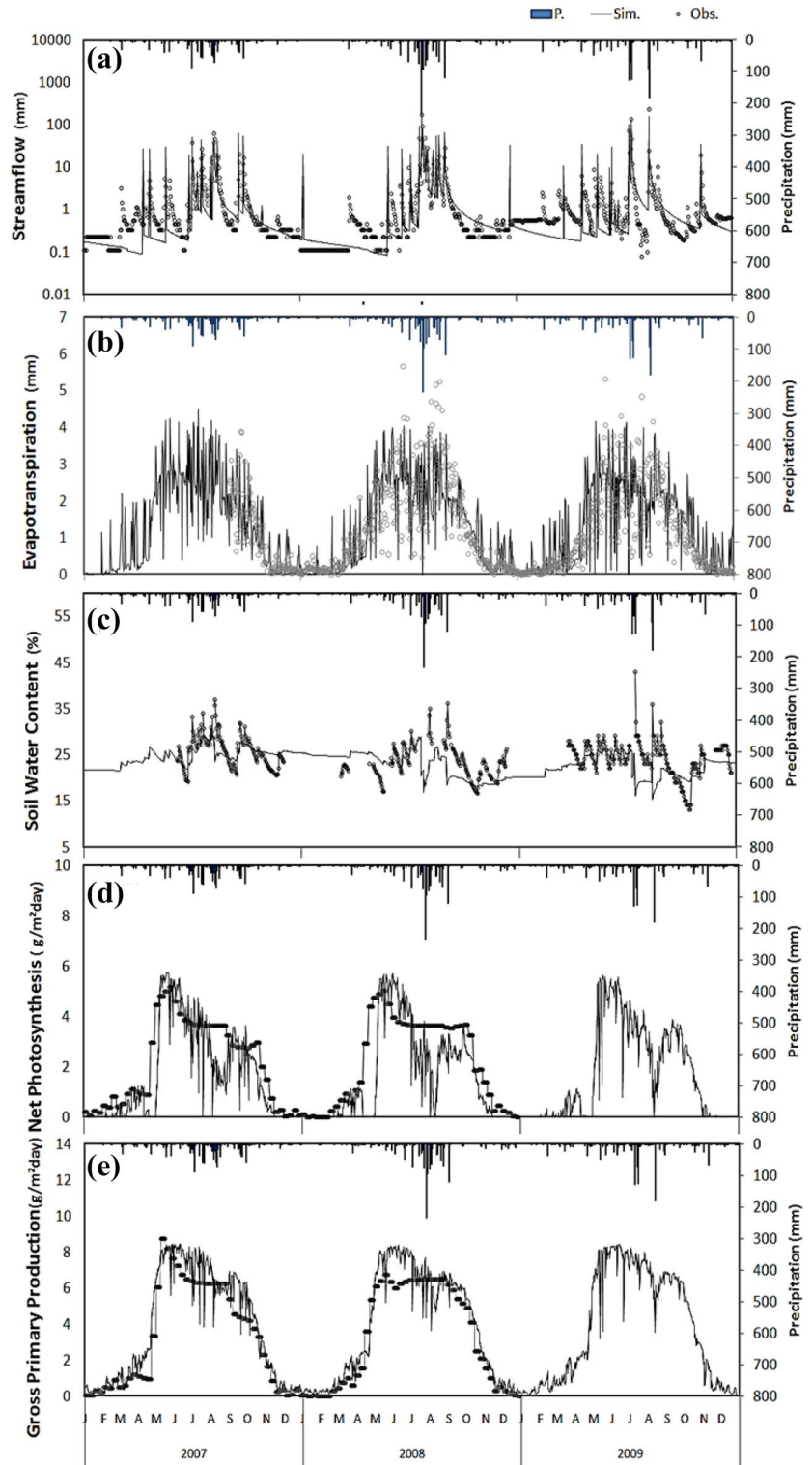

Table 7 PSNnet, GPP calibration and validation results (Shin et al. [2012b](#))

Period	P (mm/y)	PSNnet (gC/m^2)		GPP (gC/m^2)		R^2	
		MODIS	Sim.	MODIS	Sim.	PSNnet	GPP
2007	1262.2	780.8	524.6	1192.9	1395.8	0.55	0.93
2008	1498.3	807.7	500.0	1206.5	1373.0	0.38	0.93

Fig. 6 Prediction of seasonal evapotranspiration (**a**); Evaporation (**b**); transpiration (**c**); soil moisture (**d**); streamflow (**e**); response to climate changes from yearly baseline, 2020s, 2050s, 2080s (left: MIROC3.2; right: HadCM3)
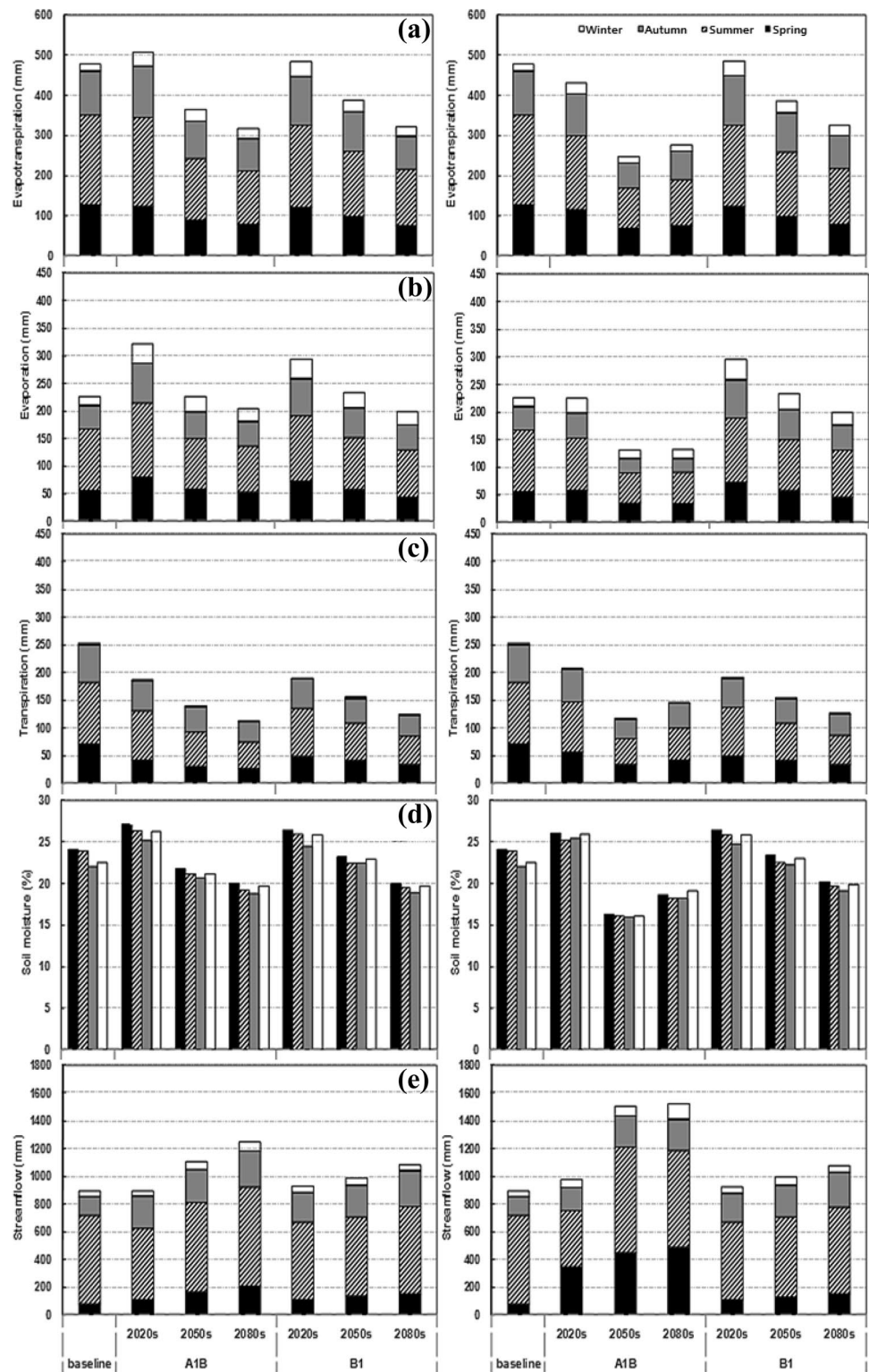
that of the A1B scenario decreased to − 54.6% in 2050. The evapotranspiration in fall decreased in every scenario except the B1 scenario in the 2020s, which increased to 11.4%. In winter, a general increase in the A1B scenario showed that the evapotranspiration in the 2050s and 2080s decreased to

− 17.1% and − 18.1%, respectively, while that in the B1 scenario in the 2020s increased to 99.0%.

The RHESSys model can generate evapotranspiration values when considering either evaporation or transpiration. The current and future change rates when considering

evaporation and transpiration are shown in Figs. 6b and 5c, respectively. For annual change rates in evaporation volume using MIROC3.2, 41.9 and 29.9% increases were shown in the 2020s in scenarios A1B and B1, respectively, and a 3.1% increase was shown in the B1 scenario in the 2050s. Annual change rates from scenario A1B in the 2050s and the 2080s in scenario B1 decreased by -0.5%, -9.9%, and -12.7%, respectively. Although evapotranspiration in these two scenarios decreased in spring and summer in the 2020s, the evaporation volume increased in the 2020s in every season. The rate of increase in the B1 winter scenario was the largest (115.5%), while that in summer was the smallest (5.5%). In the 2050s and the 2080s, the change rate in winter increased. Although several fluctuations were shown over different periods, the evapotranspiration change rate in fall increased by 69.5%.

While the evapotranspiration in spring decreased in every scenario, the evaporation volume increased in the 2020s and 2050s even though the predicted general volume decreased. Evapotranspiration in summer decreased in all scenarios, except in the 2020s, when evapotranspiration increased during all seasons. The annual evaporation rate using HadCM3 increased in the 2020s and 2050s by 30.1% and 3.0%, respectively, in the B1 scenario, but for the rest of the period, it decreased by -42.5%. In the A1B scenario, values decreased in all seasons in the 2050s and 2080s, and the change rate was the largest in summer in the 2050s (-51.6%). In the A1B scenario, the value increased in all seasons in the 2020s, except in summer, when the value was negative (-16.4%), which is similar to the change pattern in the 2050s when using MIROC3.2. Hence, the HadCM3 A1B scenario showed a higher change rate than that of MIROC3.2. The annual transpiration volume change rate of HadCM3 decreased when using MIROC3.2 from -55.4 to -24.9%, respectively, in all scenarios, and the change rate of the A1B scenario was higher than that of the B1 scenario. For seasonal patterns, the change rate in spring was the highest. The A1B change rate in the 2080s decreased by -63.8%, which is different from that in the 2020s, where evaporation increased for every season. The annual transpiration volume using HadCM3 decreased in all scenarios from -18.2 to -54.1%, and the overall value increased for all seasons. In the A1B scenario, the rate of decrease in winter was large compared to that of MIROC3.2.

As for the annual soil moisture content, those from MIROC3.2 increased by 13.2% and 10.9% in the 2020s for scenarios A1B and B1, respectively, as shown in Fig. 6d, which is a similar result to that of evapotranspiration; in other scenarios, the contents decreased by -16.3%. As in the annual comparison, the seasonal comparison showed that in the 2020s, soil moisture contents increased every season. In the A1B scenario, contents decreased every season in the 2050s and 2080s, especially in summer, when the

change rates were the largest (-11.5% and -19.8%, respectively). In the B1 scenario, the value decreased by -3.8% and -6.0% in the 2050s in spring and summer but increased by 2.1% and 1.6% in fall and winter, respectively. In the 2080s, the value decreased by 18.5% in summer, which was the largest change rate. For HadCM3, the decrease rate in scenario A1B was larger than that when using MIROC3. Particularly in the 2050s, the decrease rate in scenario A1B was -30.6%, which was the most significant change among the climate change scenarios, and that of scenario B1 in the 2050s was -1.6%, which was the smallest decrease rate. For MIROC3.2, an increase in the 2020s and a decrease in other periods were observed. The decreasing pattern in summer was also similar to that of evapotranspiration, where the decrease rate in spring was larger than that in other seasons. Because the decrease in soil moisture content directly affects the growth of farm products, and domestic sowing is accomplished in spring, measuring the lack of soil moisture content needs to be considered in the future.

Finally, annual and seasonal changes in runoff, which is the most important element in watershed hydrology, are shown in Fig. 6f. For MIROC3.2, the A1B scenario showed a change rate increase of 0.1% in 2020 and 39.6% in 2080. For seasonal changes in runoff, the MIROC3.2 results increased from 43.1 to 114.2% in spring and 52.2 to 84.3% in fall. The summer values decreased in the A1B scenario in 2020 and in the B1 scenario for all periods at rates of -19.8% and -1.1%, respectively. In winter, the value increased by 60.9% for almost all seasons. For HadCM3, the annual runoff increased from 3.6 to 70.4%, and the runoff volume increased in every season, except for summer. In A1B scenario specifically, runoff in spring increased by 551.2%, and the rates of increase in spring and fall were high in the B1 scenario.

The effects of future climate and forest vegetation changes on GPP and PSNnet

The annual and seasonal PSNnet and GPP values in the watershed, which were simulated by the RHESSys model for future climate changes, were analyzed, and the results are presented in Fig. 7.

For the annual PSNnet (Fig. 7a), the MIROC3.2 decreased from -4.1 to -69.2%, which decreased further (-84.2%) in all seasons, except in winter in the 2020s. The summer change rate was the highest. For HadCM3, the change rate of annual PSNnet ranged from -38.1 to -75.7%, which indicated that the decrease rate was larger than that of MIROC3.2. Seasonal change patterns were similar to those of MIROC3.2, and the rate decreased by -97.5%.

For MIROC3.2, the annual GPP (Fig. 7b) increased in every scenario, and the change rate ranged from 7.3 to
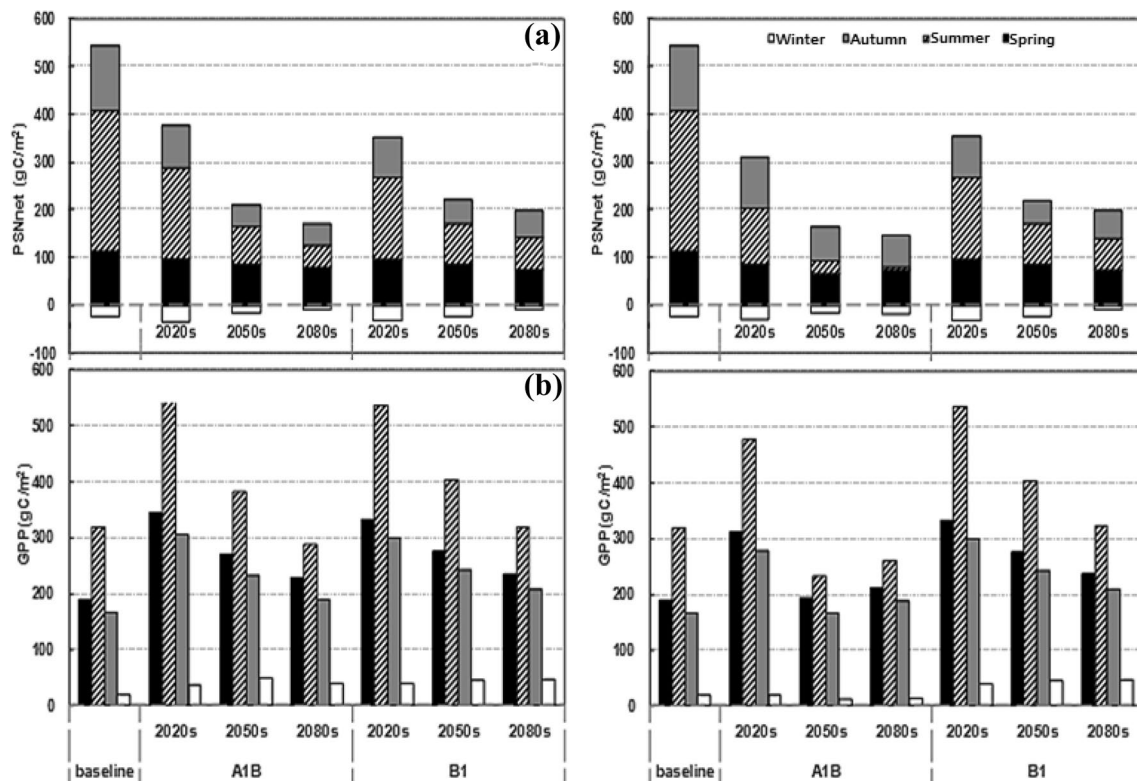
Fig. 7 Prediction of seasonal PSNet (**a**) and GPP (**b**) in response to climate changes (left: MIROC3.2; right: HadCM3)

80.3%. As time progressed, the decrease rate became larger in both scenarios. For A1B, the rate of increase was 81.8% in spring in the 2020s and 20.7% in the 2080s. In summer, the change ranged from 76.9 to − 10.0%, and in fall, the increase rate gradually decreased from 80.3% in the 2020s to 14.0% in the 2080s. In winter, the increase rate in the 2050s was the largest (157.9%). In the B1 scenario, the rate of increase in the 2020s was the largest, but it decreased gradually as time progressed. The HadCM3 pattern was similar to that of MIROC3.2 regarding the B1 scenario. In the A1B scenario, the value decreased in winter in the 2020s by − 0.2%, and it continued to decrease further as time progressed. For the A1B scenario, the largest increase rate in the 2020s was lower than that in other scenarios. The annual GPP in summer and winter decreased in the 2040s and 2080s.

Summary and conclusions

This study applies the Regional Hydroecological Simulation System (RHESSys) model, which comprehensively simulates carbon and water circulations in the ecosystem by considering interactions among the atmosphere, plants, and soils, to the Seolmacheon catchment (8.5 km^2) to predict the vegetation distributions in the 2020s, 2050s, and 2080s. The purpose of this study is to analyze the effects of future

climate changes on hydrological patterns and ecological circulations over forest watersheds. The results are summarized as follows:

After the calibration of daily runoff, PSNnet, and GPP from 2007 to 2008, the coefficients of determination ranged from 0.59 to 0.93.

For seasonal changes in temperature as a result of future climate changes, MIROC3.2 increased for all four seasons, while HadCM3 drastically decreased from − 41.0% (− 1.0 °C) to − 25.1% (− 0.6 °C) in winter in the 2020s and 2050s; precipitation increased in all scenarios.

The hydrological evaluation of the watershed, which was conducted by simulating the RHESSys model for each climate change scenario, showed that evapotranspiration and soil moisture content increased in the 2020s for all scenarios then gradually decreased in the latter part of the study period as runoff increased.

When analyzing the dependence of PSNnet on climate changes, the rate decreased from − 34.1 to − 69.2% when using MIROC3.2. The rate decreased by − 84.2% in the 2020s for all seasons (except winter). The rate of change in summer was especially high. For HadCM3, the rate of change in the annual PSNnet ranged from − 38.1 to − 75.7%, which indicate that the rate of decrease was higher than that of MIROC3.2. Seasonal change patterns were similar to those of MIROC3.2, and the rate decreased by − 97.5%.

Annual GPP from the MIROC3.2 increased in all scenarios, and the rate of change ranged from 7.3 to 80.3%. In both scenarios, the rate of decrease increased as time progressed. HadCM3 was similar to MIROC3.2 in the B1 scenario in regard to annual GPP, but in A1B, the value decreased in winter in the 2020s by -0.2%, which further decreased as time progressed. In the A1B scenario, the largest rate of increase in the 2020s was far smaller than that in other scenarios. The annual GPP and the GPP in summer and winter in the 2040s and 2080s decreased.

Because the movement of plants is slower than that of climate zones due to temperature increases, the projected decrease in evapotranspiration in existing forests should remain in the minimal state or potentially wither and die due to heat stress, droughts, and fires (in an extreme case). The simulation results show that local plants withering away cause the average annual temperature to increase by as much as 2.6–3.6 °C.

References

Band LE, Patterson P, Nemani R, Running SW (1993) Forest ecosystem processes at the watershed scale: incorporating hillslope. Agric For Meteorol 63:93–126

Baron JS, Hartman MD, Kittel TGF, Band LE, Ojima DS, Lammers RB (1998) Effects of land cover, water redistribution, and temperature on ecosystem processes in the South Platte basin. Ecol Appl 8(4):1037–1051

Beven K, Kirkby M (1979) A physically-based variable contributing area model of basin hydrology. Hydrol Sci Bull 24:43–69

Cao M, Woodward FI (1998) Net primary and ecosystem production and carbon stocks of terrestrial ecosystem and their response to climate change. Glob Change Biol 4:185–198

Clapp R, Hornberger G (1978) Empirical equations for some soil hydraulic properties. Water Resour Res 14:601–604

Creed IF, Tague C, Swanson R, Rothwell RL (2000) The potential impacts of harvesting on the hydrologic dynamics of boreal watersheds. In: Proceedings of American Geophysical Union 2000 Spring Meeting, Washington, D.C., American Geophysical Union

Dan L, Ji J, Xie Z, Chen F, Wen G, Richey JE (2012) Hydrological projections of climate change scenarios over the 3H region of China: a VIC model assessment. J Geophys Res 117:D11102

Farquhar GD, von Caemmerer S (1982) Modeling photosynthetic response to environmental conditions. Encyclopedia of plant physiology. Physiological plant ecology II: water relations and carbon assimilation; encyclopedia of plant physiology. New Series 12B:549–587

Fredeen AL, Randerson JT, Holbrook NM, Field CB (1997) Elevated atmospheric CO_2 increased water availability in a water-limited grassland ecosystem. J Am Water Resour Assoc 33:1033–1039

Heinsch FA, Reeves M, Votava P, Kang S, Milesl C, Zhao M, Glassy J, Jolly WM, Loehman R, Bowker CF, Kimball JS, Nemani RR, Running SW (2003) User's guide, GPP and NPP(MOD 17A2/A3) products NASA MODIS land algorithm. The University of Montana, Missoula

Hwang TH, Kang SK, Kim YI, Kim J, Lee DW, Band LE (2008) Evaluating drought effect on MODIS gross primary production (GPP) with an eco-hydrological model in the Mountainous Forest, East Asia. Glob Change Biol 14(5):1037–1056

IPCC (2007) Climate change 2007: the physical science basis, contribution of working group 1 to the 4th assessment report of the intergovernmental panel on climate change. In: Salomon S, Qin D, Manning M, Chen Z, Marquis M, Averyt KB, Tignor M, Miller HL (eds) Cambridge University Press, Cambridge, United Kingdom

Ito A, Oikawa T (2000) A model analysis of the relationship between climate perturbations and carbon budget anomalies in global terrestrial ecosystems: 1970 to 1997. Clim Res 15(3):161–183

Jarvis P (1976) The interpretations of the variations in leaf water potential and stomatal conductance found in canopies in the field. Philos Trans R Soc Lond B273:593–610

Joh HK, Lee JW, Shin HJ, Park GA, Kim SJ (2010) Evaluation of evapotranspiration and soil moisture of SWAT simulation for mixed forest in the Seolmacheon catchment. Korean J Agric For Meteorol 12(4):289–297 **(in Korean with English abstract)**

Joh HK, Lee JW, Park M, Shin HJ, Yi JE, Kim GS, Srinivasan R, Kim SJ (2011) Assessing climate change impact on hydrological components of a small forest watershed through SWAT calibration of evapotranspiration and soil moisture. Trans ASABE 54(5):1773–1781

Kelliher FM, Leuning R, Raupach MR, Schulze ED (1995) Maximum conductances for evaporation from global vegetation types. Agric For Meteorol 73:1–16

Knapp AK, Hamerlynck EP, Ham JH, Owensby CE (1996) Responses in stomatal conductance to elevated CO_2 in 12 grassland species that differ in growth form. Vegetatio 125:31–41

Korea Institute of Construction Technology (2008) Development of watershed Assessment techniques for healthy water cycle. Summary report, Korea Institute of Construction Technology, 2008–2039, pp 97–101. **(in Korean)**

Kwon HJ, Lee H, Lee YK, Lee JW, Jung SW, Kim J (2009) Seasonal variations of evapotranspiration observed in a mixed forest in the Seolmacheon catchment. Korean J Agric For Meteorol 11(1):39–47 **(in Korean with English abstract)**

Körner C (1995) Leaf diffusive conductances in the major vegetation types of the globe. In: Schulze ED, Caldwell MM (eds) Ecophysiology of photosynthesis. Springer, New York, pp 463–490

López-Moreno JI, Zabalza J, Vicente-Serrano SM, Revuelto J, Gilaberte M, Azorin-Molina C, Morán-Tejeda E, García-Ruiz JM, Tague C (2014) Impact of climate and land use change on water availability and reservoir management: scenarios in the Upper Aragon River, Spanish Pyrenees. Sci Total Environ 493:1222–1231

Lüdeke M, Badeck F, Otto R (1994) The Frankfurt biosphere model: a global process oriented model of seasonal and long-term CO_2 exchange between terrestrial ecosystems and the atmosphere. I. Model description and illustrative results for cold deciduous and boreal forests. Clim Res 4:143–166

Lutze JL, Gifford RM (1998) Carbon accumulation, distribution and water use of Danthonia richardsonii swards in response to CO_2 and nitrogen supply over four years of growth. Glob Change Biol 4:851–861

Minville M, Brissette F, Krau S, Leonte R (2009) Adaptation to climate change in the management of a Canadian water-resources system exploited for hydropower. Water Resour Manag 23:2965–2986

Monteith JL (1965) Evaporation and environment. In: 19th symposia of the society for experimental. Biology, vol 19, pp 205–234

Morgan JA, LeCain DR, Read JJ, Hunt HW, Knight WG (1998) Photosynthetic pathway and ontogeny affect water relations and the

impact of CO_2 on *Bouteloua gracilis* (C4) and *Pascopyrum smithii* (C3). Oecologia 114:483–493

Nash JE, Sutcliffe JV (1970) River flow forecasting through conceptual models, part I-A discussion of principles. J Hydrol 10:283–290

Nemani RR, Keeling CD, Hashimoto H, Jolly WM, Piper SC, Tucker CJ, Myneni RB, Running SW (2003) Climate-driven increases in global terrestrial net primary production from 1982 to 1999. Science 300:1560–1563

Park JS, Kim KT, Lee JH, Lee KS (2006) Applicability of multi-temporal MODIS images for drought assessment in South Korea. Korean Assoc Geogr Inf Stud 9(4):176–192 **(in Korean with English abstract)**

Park JY, Park GA, Kim SJ (2013) Assessment of future climate change impact on water quality of Chungju Lake, South Korea, Using WASP Coupled with SWAT. J Am Water Resour Assoc 49(6):1225–1238

Parton W, Mosier A, Ojima D, Valentine D, Schimel D, Weier K, Kulmala A (1996) Generalized model for N_2 and N_2O production from nitrification and denitrification. Global Biogeochem Cycles 10:401–412

Rawls WJ, Brakensiek DL, Saxton KE (1982) Estimation of soil water properties. Trans. ASAE 108:1316–1320

Running S, Coughlan J (1988) A general model of forest ecosystem processes regional applications, hydrologic balance, canopy gas exchange and photosynthesis. Can J For Res 17:472–478

Running S, Nemani R, Hungerford R (1987) Extrapolation of synoptic meterological data in mountainous terrain and its use for simulating forest evapotranspiration and photosynthesis. Can J For Res 17:472–483

Running SW, Thornton PE, Nemani R, Glassy JM (2000) Global Terrestrial gross and net primary productivity from the earth observing system. In: Sala OE, Jackson RB, Mooney HA, Howarth RW (eds) Methods in ecosystem science, Springer, New York, pp 44–57

Running SW, Nemani RR, Heinsch FA, Zhao M, Reeves M, Hashimoto H (2004) A continuous satellite-derived measure of global terrestrial primary production. Bioscience 54(6):547–560

Schulze ED, Kelliher FM, Körner C, Lloyd J, Leuning R (1994) Relationships among maximum stomatal conductance, ecosystem surface conductance, carbon assimilation rate and plant nitrogen nutrition: a global ecology scaling exercise. Annu Rev Ecol Syst 25:629–660

Shi X, Mao J, Thorton PE, Hoffman FO, Post WM (2011) The impact of climate CO_2, nitrogen deposition and land use change on simulated contemporary global river flow. Geophys Res Lett 38(8):L08704

Shi X, Mao J, Thornton PE, Huang M (2013) Spatiotemporal patterns of evapotranspiration in response to multiple environmental factors simulated by the community land model. Environ Res Lett 8(024012):12

Shin HJ, Ha R, Park M, Kim SJ (2010) Estimation of Spatial Evapotranspiration using the Relationship between MODIS NDVI and Morton ET: For Chungjudam Watershed. J Korean Soc Agric Eng 52(1):19–24 **(in Korean with English abstract)**

Shin HJ, Park GA, Park M, Kim SJ (2012a) Projection of forest vegetation change by applying future climate change scenario MIROC3.2 A1B. Korean Assoc Geogr Inf Stud 15(1):64–75 **(in Korean with English abstract)**

Shin HJ, Park M, Kim SJ (2012b) Evaluation of forest watershed hydro-ecology using measured data and RHESSys model: For the Seolmacheon Catchment. J Korea Water Resour Assoc 45(12):1293–1307 **(in Korean with English abstract)**

Shin HJ, Park M, Hwang SJ, Park JY, Kim SJ (2014) Hydrologic impact of climate change with adaptation of vegetation community in a forest-dominant watershed. Paddy Water Environ 12(s1):s51–s63

Tague CL, Band LE (2001) Simulating the impact of road construction and forest harvesting on hydrologic response using rhessys. Earth Surf Process Landf 26:135–151

Tague CL, Band LE (2004) RHESSys: regional hydro-ecologic simulation system-an object oriented approach to spatially distributed modeling of carbon, water, and nutrient cycling. Earth Interact 8:1–42

Vertessy RA, Hatton TJ, Benyon RJ, Dawes WR (1996) Long term growth and water balance predictions for a mountain ash (*Eucalyptus regnans*) forest catchment subject to clear felling and regeneration. Tree Physiol 16:221–232

Volk M, Niklaus PA, Korner C (2000) Soil moisture effects determine CO_2 responses of grassland species. Oecologia 125:380–388

Watson FGR, Pierce LL, Mulitsch M, Newman W, Nelson J, Rocha A (1999) Spatial modelling of the impacts of 150 years of land use change on the carbon, nitrogen, and water budgets of a large watershed. In: ESA annual meeting, 8th–12th August 1999, Spokane, USA

White MA, Thornton PE, Running SW, Nemani RR (2000) Parameterization and sensitivity analysis of the BIOME–BGC terrestrial ecosystem model: net primary production controls. Earth Interact 4(3):1–85

Yang D, Shao W, Yeh PJF, Yang H, Kanae S, Oki T (2009) Impact of vegetation coverage on regional water balance in the nonhumid regions of China. Water Resour Res 45:W00A14

Zierl B, Bugman H, Tague CL (2006) Water and carbon fluxes of European ecosystem: an evaluation of the ecohydrological model RHESSys. Hydrol Process 214(24):3328–3339